Review

Electrospray–differential mobility analysis of bionanoparticles

Suvajyoti Guha[1,2], Mingdong Li[1,2], Michael J. Tarlov[2] and Michael R. Zachariah[1,2]

[1] University of Maryland, College Park, MD 20742, USA
[2] National Institute of Standards and Technology, Gaithersburg, MD 20899, USA

Electrospray–differential mobility analysis (ES–DMA) is a versatile technique used to aerosolize bionanoparticles and measure their electrical mobility at ambient conditions. ES–DMA is similar to electrospray–mass spectrometry (ES–MS), but measures the effective particle size, rather than mass. It has a wide range of applications and nominally can be used to characterize biomolecules and nanoparticles ranging in size from a few nanometers (~3 nm) to several hundred nanometers, to obtain multimodal size distributions in minutes. Although both the ES and the DMA are mature technologies, they are finding increased use in combination to characterize particles in liquids. In this paper, we review ES–DMA, and how it has recently been used to characterize bionanoparticles such as polymers, proteins, viruses, bacteriophages and nanoparticle–biomolecule conjugates.

Historical background on electrospray–differential mobility analysis (ES–DMA)

The field of bionanotechnology has undergone explosive growth in the last decade that has spurred the development of new analytical techniques for their characterization. One such method, ES–DMA, is a technique that couples an ES source (see Glossary) with an ion mobility spectrometer. ES was used initially for applications involving surface coatings, agricultural treatments, emulsions and as colloidal micro-thrusters [1]. In the 1980s, it was discovered that ES could be used for aerosolizing biomacromolecules allowing their analysis by mass spectrometry (MS) [2]. DMA is just one of several ion mobility techniques, and its conceptualization can be traced to the late 19th–early 20th century [3]. In general, all ion mobility techniques measure how fast an ion moves in a viscous medium under the influence of an electrical field, and depending on the design, can probe particle sizes from sub-nanometer to several hundred micrometers. The predecessor of the present day DMA was developed in 1957 to investigate charging of small particles. This DMA, further modified in 1970s, was subsequently commercialized [3].

Although exploratory experiments were underway as far back as 1994 [4], the first integration of ES with DMA to analyze biomolecules, can be traced back to 1996, when this technique was used to determine the size of globular proteins [5]. Subsequently, researchers have used ES–DMA to characterize other bionanoparticles including polymers, viruses, bacteriophages, nanoparticle–bionanoparticle and bionanoparticle–bionanoparticle conjugates, leading to a rapid increase in the number of publications reporting its use (Box 1). Although some groups have presented short reviews of the method and its application to specific bionanoparticles [6–9], here we provide a comprehensive review of the applications of the ES–DMA to a wide variety of bionanoparticles. In this context, bionanoparticles are defined as nano-sized particles that are either biologically or synthetically-derived or are functionalized to integrate into a biological context. Space constraints limit us from discussing non-functionalized inorganic nanoparticles such as gold, silver, etc, which have found use in biomedical applications.

Principles of the ES–DMA

The mobility velocity (v) of a charged particle is proportional to the electrical field (E):

$$v = ZE \tag{1}$$

where Z is a proportionality constant and is called the electrical mobility [10]. Although Z is nominally considered a constant independent of electric field, under some conditions of high field, asymmetric particles can align and change their mobility [11]. This latter point will not be considered in this review. The electrical mobility can be derived through a balance of the electrical force and the

Glossary

Analytical ultracentrifugation (AUC): a technique to separate particles in solution based on the differences of centrifugal forces.
Condensation particle counter (CPC): used for aerosol particle counting, usually placed after ES–DMA.
Dynamic light scattering (DLS): a technique to determine the hydrodynamic radius of particles in solution based on the intensity of scattered light.
Differential mobility analyzer (DMA): selects nano-sized particles based on the balance of drag and electrical forces at atmospheric pressure. Alternative names for DMA include ion mobility spectrometer (IMS), scanning mobility particle spectrometer (SMPS), gas phase electrophoretic molecular mobility analyzer (GEMMA) and electrical aerosol analyzer (EAA).
Electrospray (ES): a method for generating very fine charged aerosols by passing a conductive solution through a capillary held at a high potential. Alternative names for ES include nano-electrospray (n-ES), electrospray ionization (ESI), electro-hydrodynamic atomization (EHDA) and electrospray aerosol generator (EAG).
Electrospray–differential mobility analysis (ES–DMA): alternative names include nES-GEMMA, integrated virus detection system (IVDS), macro-IMS and ES–SMPS.
Field-flow fractionation (FFF): a technique to separate particles in solution based on their mobilities in the liquid phase under the influence of gravitational field, electric field, etc.
Size exclusion chromatography (SEC): a technique to separate particles in solution based on their interaction time with a column.

Corresponding author: Zachariah, M.R. (mrz@umd.edu).
Keywords: electrospray-differential mobility analysis; viruses; proteins; gold-protein conjugates.

Box 1. Publication statistics for ES–DMA for bionanoparticle characterization

As already mentioned in the main text, the first reported application of ES–DMA to biological molecules was for characterizing proteins [5]. This work was followed over the next decade by several reports related to characterization of several other proteins [15], viruses [43] and polymers [18]. Starting in 2006, a dramatic increase in the number of publications (Figure Ia) and citations (Figure Ib) related to ES–DMA occurred with contributions from several different groups [13,30,39,46,54,55,73].

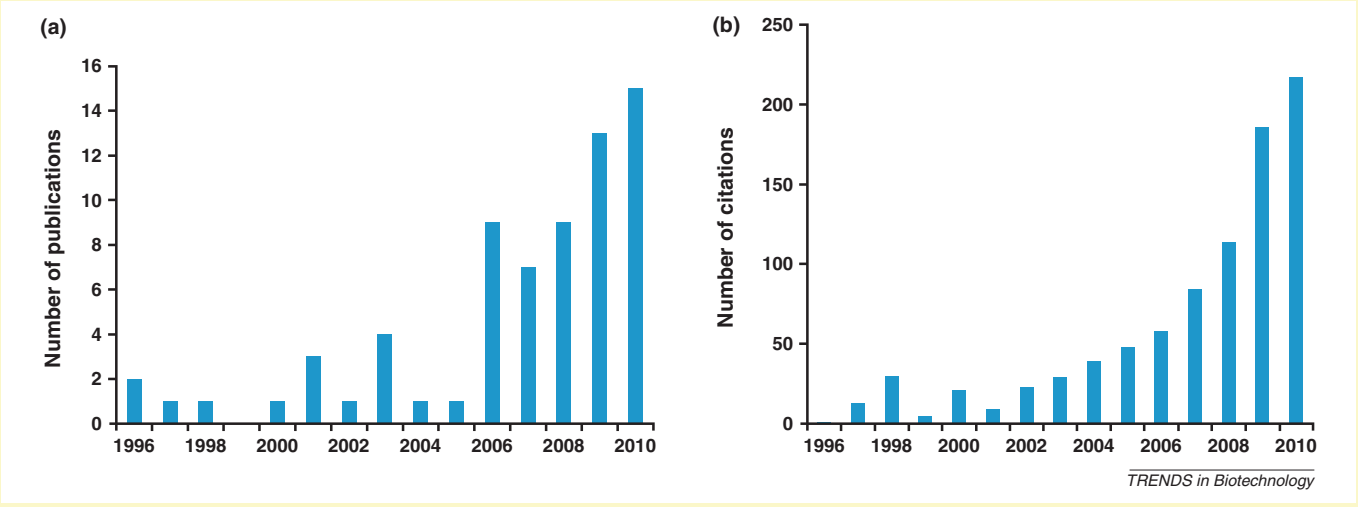

Figure I. Popularity trends of ES–DMA. **(a)** Published articles on ES–DMA from 1996 to 2010, using the key words 'electrospray' and 'differential mobility analysis' in Web of Knowledge (version 5.3), and **(b)** number of citations (including self-citations) from 1996 to 2010.

drag force [10]. Under this constraint the electrical mobility is given by:

$$Z \propto \frac{C_c(D_m)}{D_m} \quad (2)$$

where D_m is the mobility equivalent *spherical* diameter of a particle, C_c is the Cunningham slip factor [10], which corrects for the non-slip boundary condition employed in the development of the drag force (Stokes' law). For particles smaller than the mean free path of the gas (~66 nm at 293 K and 100 kPa), C_c is inversely proportional to D_m, and for larger particles decreases linearly with increasing particle diameter. Thus, for very small particles (<50 nm), the DMA separates particles based on differences in projected area, whereas for larger particles (>100 nm) separation is based on differences in diameter.

There are many types of analyzers for mobility classification, which fall broadly into two classes: time-of-flight and differential mobility [3,10]. Although the former separates particles temporally, the latter separates particles spatially. There are other available varieties of mobility classifiers such as high field asymmetric ion mobility and travelling voltage wave ion mobility, but these more specialized techniques are not discussed here. For a brief overview of these techniques, the reader is directed to reference [12]. Within the class of DMAs, the cylindrical configuration is the most widespread, primarily because its electrodes can be manufactured with exacting spatial specifications, and thus, electric fields are highly uniform and precisely controlled. The cylindrical DMA consists of two electrodes, one that is held at a high voltage (usually the inner electrode), and another that is grounded (usually the outer cylinder). As shown in Figure 1, a flow of the analyte in the form of polydispersed aerosols, and the laminar sheath flow gas (Q_{sh}) (usually air or nitrogen) enter the annular region of the DMA, where the charged particles move with an electrophoretic velocity described by Equations 1 and 2. For a given applied voltage (V), and Q_{sh}, a given mobility (Z) can be extracted from the instrument and counted [10]:

$$Z = g(Q_{sh}, V, DMA_{design}) \quad (3)$$

Thus by scanning the DMA voltage from low to high, the mobility of particles from subnanometer size to several hundred nanometers can be obtained, depending on DMA design. Then, by substituting Equation 3 in Equation 2, the mobility diameter, D_m of a particle can be determined. One major constraint is that the sheath flow must remain laminar, such that the only forces (electrostatic and drag) acting on the particles are in the radial direction.

Because the DMA operates in the aerosol phase, the analyte of interest needs to be dispersed in a gas. This is commonly achieved through the ES process, which aerosolizes nanoparticles (bio and non-bio alike) at room temperature. By applying a high voltage to the analyte solution, the fluid exiting the fused silica capillary disintegrates by electrostatic repulsion to generate a mist of finely mono-dispersed and multiply charged droplets, as shown in Figure 1. It is possible at this point to evaporate the droplets and pass the resulting dried charged analyte particles directly to the DMA [13,14]. More commonly, however, the analyte particles are passed through a 'neutralizer' (see Figure II in Box 2), prior to the DMA. The 'neutralizer' is an ionizing radiation source (e.g. Po-210), which ionizes the carrier gas and reduces the net charges on the particles through a diffusion charging mechanism. The advantage of doing this is that a known Fuchs'-Boltzmann distribution of charges can be placed on the particles. A complete size distribution (Figure 1), also called a mobility spectrum, can be obtained by scanning the applied

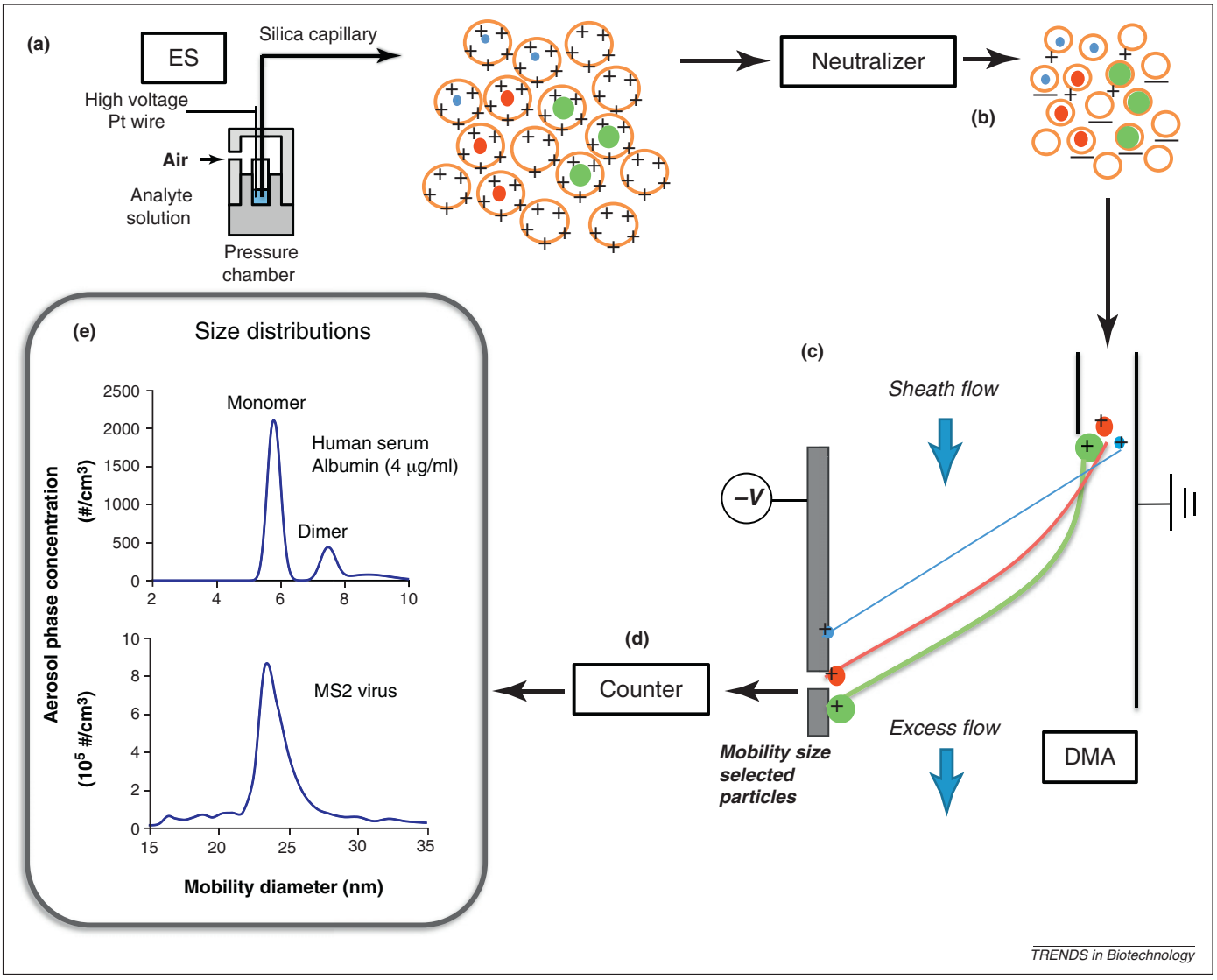

Figure 1. Schematic of the different components of the electrospray–differential mobility analysis (ES–DMA) system. **(a)** The analyte, typically dissolved in a volatile buffer solution, is passed through a fused silica capillary under pressure and then electrosprayed to produce multiply charged droplets containing the analyte. The ES in this figure is shown operating in the positive ion mode. The analyte containing droplets are then mixed with air (sometimes also supplemented with CO_2) and are passed through the neutralizer **(b)** where solvent from droplets continue to evaporate, and a residual charge on the particles results from diffusion charging from positively and negatively charged ions (see Figure II in Box 2). **(c)** Only positively (or negatively) charged particles are then classified by applying a negative (or positive) bias in the DMA and eventually counted. The remainder of the particles with zero or negative (or positive) charges will collide with one of the electrodes of the DMA and be lost. (More detailed descriptions of the mechanism of how ES droplets evaporate and charge is transferred to the analyte are provided elsewhere [65,66].) **(d)** Analyte particles are eventually detected by either using a condensation particle counter or an electrometer, and thus a size distribution is obtained. **(e)** The size distributions of human serum albumin and MS2 virus. Size distributions adapted, with permission, from [5] and [46]. One of the outstanding features of the ES–DMA is that the detector or counter can be easily removed and the DMA can be set at a particular voltage to collect size selected particles on transmission electron microscopy (TEM) grids or in aqueous solution [6].

voltage while counting particles exiting the DMA. Note that the DMA is only a band pass filter, and thus requires a detector, such as an electrometer (because particles are charged), or a condensation particle counter (CPC) (see Figure IV in Box 2). More detailed descriptions of the experimental conditions and parameters are given elsewhere [5,15,16].

Polymers and proteins

Almost all polymers and proteins of interest are amenable to characterization by ES–DMA, which offers faster characterization times over size exclusion chromatography (SEC), analytical ultracentrifugation (AUC), flow-field fractionation (FFF) and gel electrophoresis, in addition to providing a direct measure of size. Although having much better resolution compared to ES–DMA, ES–MS methods are not routinely used for measuring very high molecular weight proteins (>300 kDa) and the presence of more than one charge state can complicate data interpretation [17].

The first application of ES–DMA to nucleic acids can be traced back to 1997 when it was used for determining the mobility diameter of single-stranded and double-stranded DNA from 6 kDa to 900 kDa [18]. Further, in 2004, polyethylene glycols (PEGs) in the size range of 4 to 700 kDa were used to establish that molecular weight and mobility diameter could be correlated by a one-third power law [19], a correlation that had already been established for proteins 3 years prior [15]. Similar behavior has been reported for water-insoluble polymers [20]. Using this

correlation, the ES–DMA can also been used to determine density of polymers (or proteins) [7,15].

$$\rho = \frac{6MW}{N_{avg}\pi d_{DMA}^3} \quad (4)$$

Here, ρ is the density of the polymer (or protein), MW is the molecular weight, N_{avg} is the Avagadro's number and d_{DMA} is the analyte diameter determined by the DMA [6,18]. It should be pointed out that for a known particle density, Equation 4 can conversely also be used to determine the molecular weight. Such a correlation is obvious for any globular particle as it resembles a sphere. However, the correlation seems to work even for non-spherical polymers such as PEG, probably because the ES droplet evaporation results in a compact dry particle. Using Equation 4, the densities of PEGs have been found to vary significantly (0.52–1.3 g/ml) amongst different groups [19,21]. Such a variation has also been seen for proteins and will be discussed later.

ES–DMA has been used to determine polydispersity in PEGs by assuming the density of PEGs to be the same as proteins [21]. In that study, the 2 kDa PEG monomers were

Box 2. Data processing of the ES–DMA

The raw data obtained with ES–DMA(–CPC) undergoes a series of corrections for reasons discussed below in Figures II, III and IV, to obtain the actual aerosol phase size distribution (Figure I).

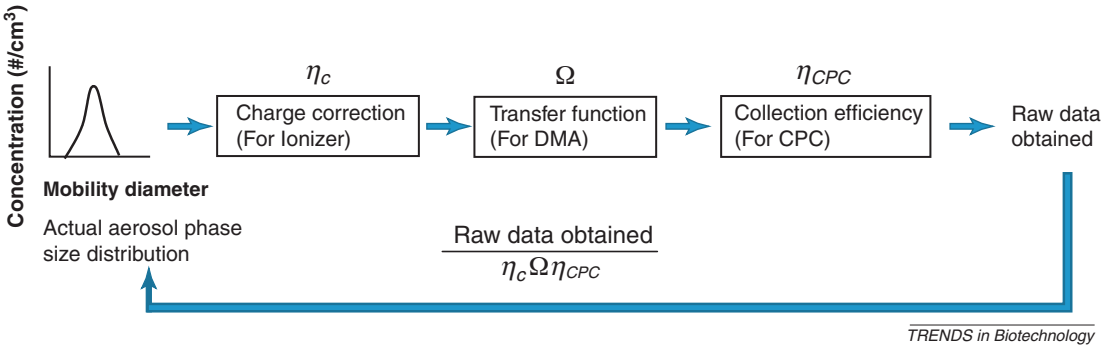

Figure I. Data processing in the ES–DMA. The raw counts are corrected for charge correction, transfer function of the DMA and collection efficiency (if a CPC is used for counting).

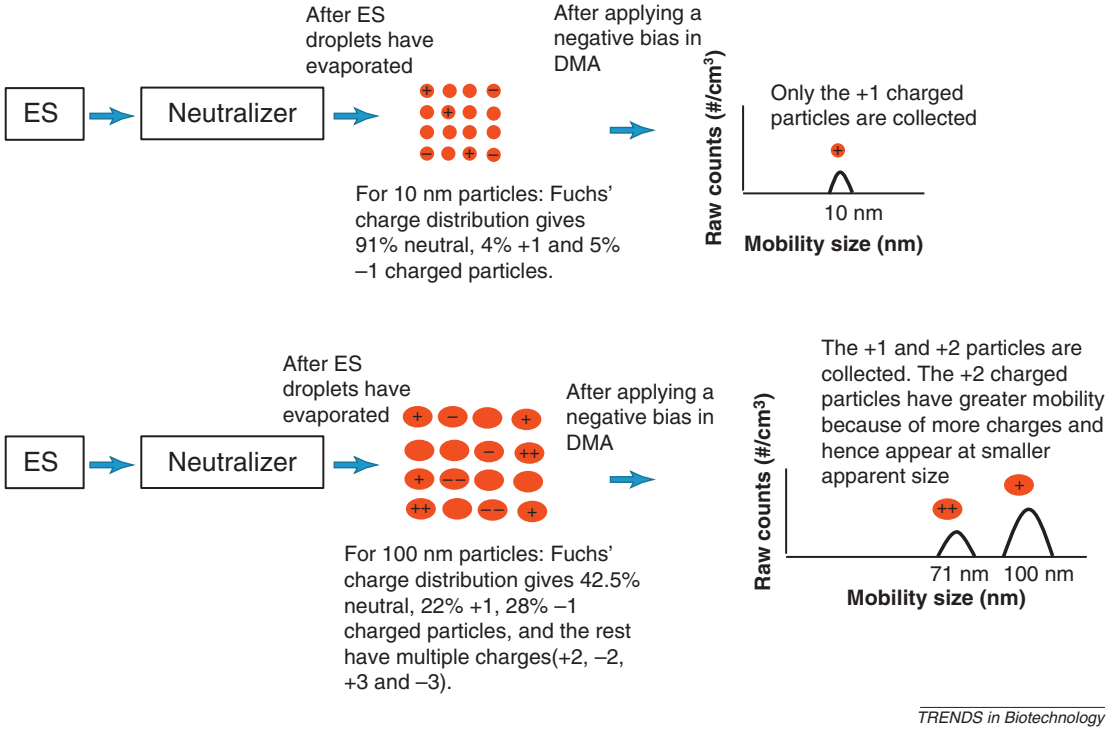

Figure II. Charge correction in the aerosol phase. Nominally, ES droplets containing analyte particles have multiple charges that are transferred to the analyte upon evaporation of the ES droplet. This process, also encountered in ES–MS, would result in multiple peaks for the same analyte [17]. To simplify the size distribution, an ionizer (usually called a neutralizer or diffusion charger) is typically used to produce a known Fuchs' charge distribution by exposing particles to gas ions produced by ionizing radiation from a radioactive source (e.g. Po-210, Kr-85). The neutralizer significantly reduces the problem of multiple charging, and thus multiple peaks for small particles (say 20–30 nm). However, this charge reduction depends on the particle size. Multiple charging is still observed for comparatively larger particles (~40 nm and greater), although to a much lesser extent relative to ES–MS. Fortunately, the distribution of the charges as a function of size is well understood, and thus determining the original analyte distribution is relatively straightforward [10]. Note that the term 'neutralizer' is a misnomer, and is rather a charge reducer.

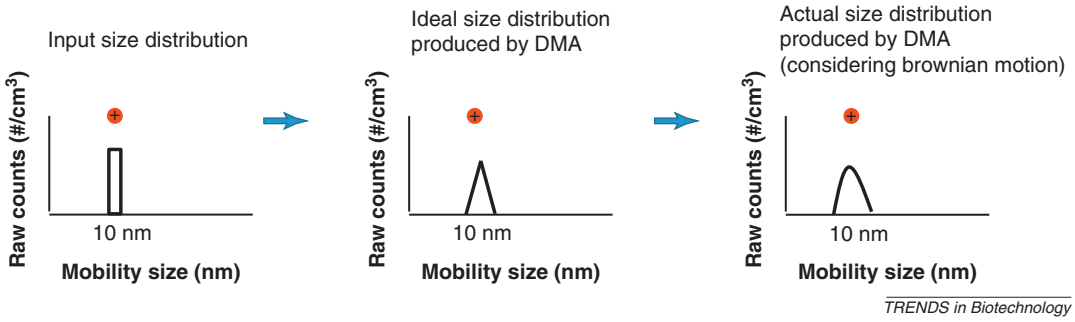

Figure III. Effect of transfer function and resolution of a DMA on size distribution. The ultimate resolution and throughput of the DMA can be described by a transfer function, which depends on the operating conditions and geometry of the DMA [10,69]. Under balanced flow conditions (i.e. when sheath flow equals excess flow and analyte or aerosol flow in equals monodispersed size selected flow out), the ratio of the sheath to the analyte flow in provides an ultimate measure of the theoretical resolution [10]. The transfer function can be further broadened by Brownian diffusion [10]. Further, when the DMA is used to obtain mobility distributions at rapid rates (a few minutes), the transfer function becomes more complex. Fortunately, the governing equations for determining the transfer function in such cases are well established and can be accounted for [10]. Based on practical sheath-to-analyte flow rates employed, the resolution of DMAs range from 10:1 to 100:1 [70], and are thus significantly lower than the resolution of most MS. A 25:1 resolution implies that a DMA is able to resolve a 10 nm particle from a particle of size $\leq$9.8 nm or $\geq$10.2 nm.

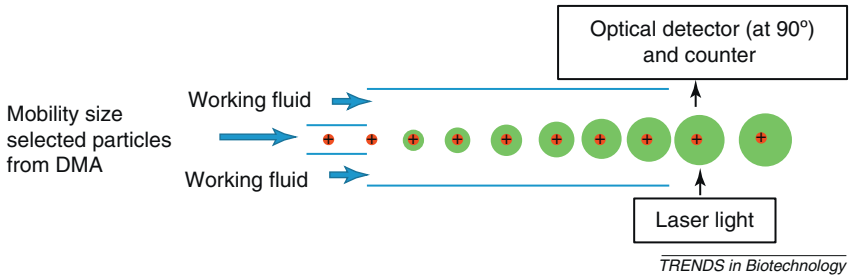

Figure IV. Working principle of the condensation particle counter (CPC). The CPC is the most sensitive detector available, and is about a thousand times more sensitive than commercially available electrometers. The high counting sensitivity of a CPC is based on condensation of a working fluid (alcohol or water) on the particle, which increases in size ($\sim$10 μm) so that it can be easily counted optically. However, although extremely sensitive, the CPC suffers from a lower size limit of detection of $\sim$2.5 nm because the droplet activation efficiency is size dependent (i.e. smaller analytes are more difficult to activate at a given supersaturation of the working fluid). This size dependence is usually accounted for by calibrating CPCs against electrometers and is called the CPC collection efficiency (η_{CPC}) [71]. It should be pointed out that modifications including use of different working fluids and operating temperatures can lower the size limit to $\sim$1 nm [72].

not observed because its size fell below the minimum detectability limit of commercial CPCs ($\sim$2.5 nm) [22]. However, this limitation can be overcome by using an electrometer instead of a CPC, if the concentration of the analyte is sufficiently high.

ES–DMA has been used to characterize different generations of poly(amido-) amine dendrimers (G2–G10) and size distributions obtained were found to be in reasonable agreement with atomic force microscopy, transmission electron microscopy and small angle X-ray or neutron scattering [23]. In this study, the densities of the dendrimers were determined to be $\sim$0.54 g/ml. It should be pointed out that for some generations of these dendrimers, the density values obtained using ES–DMA were about a factor of two smaller than the stated densities of the manufacturer. Silk-elastin-like protein polymers (SELP) are a new class of materials that can potentially be used for gene delivery applications. Recently, it has been demonstrated with the ES–DMA that such polymers can be electrosprayed to produce finely-tunable, potentially non-toxic nanoparticles either by changing concentration of the SELPs in solution or by changing solution viscosities [24].

Another potentially valuable application of ES–DMA is characterizing and quantifying proteins and protein aggregates, the latter being a common problem during therapeutic protein development or storage [25]. ES–DMA possesses some distinct advantages relative to other more popular techniques such as SEC, dynamic light scattering (DLS) and FFF. For example, in SEC, trimers-tetramers-pentamers and larger immunoglobulin aggregates elute together, and thus cannot be distinguished, but can be easily characterized with ES–DMA [26]. In DLS, the intensity of light scattering scales as the sixth power of the hydrodynamic diameter. Thus, it cannot characterize heterogeneous populations unless the size difference between the particles is at least >3:1. By contrast, ES–DMA size selects either on the basis of the inverse of projected area (e.g. 10 nm particles), or equivalent diameter (e.g. 100 nm particles) and thus has no such constraint. Further, ES–DMA has a limit of detection that is about 1000-fold lower compared to techniques that use UV detectors such as SEC, AUC and FFF [4]. The first reported use of ES–DMA [5] employed several different globular proteins from a molecular weight of 5.7 kDa (bovine pancreas insulin) to 669 kDa (bovine thyroglobulin). It was demonstrated that the monomers of different proteins can be differentiated from their respective oligomers (dimers, trimers), and that there was a strong correlation between the molecular weight and the mobility diameter. This molecular weight–mobility diameter empirical correlation (Figure 2) has been confirmed by several groups for both globular as well as non-globular proteins ranging from a few kDa [15,16,27,28] to several MDa [28]. Recalling that the DMA does not measure mass directly, but rather projected area (for particles smaller than the gas mean free path), the

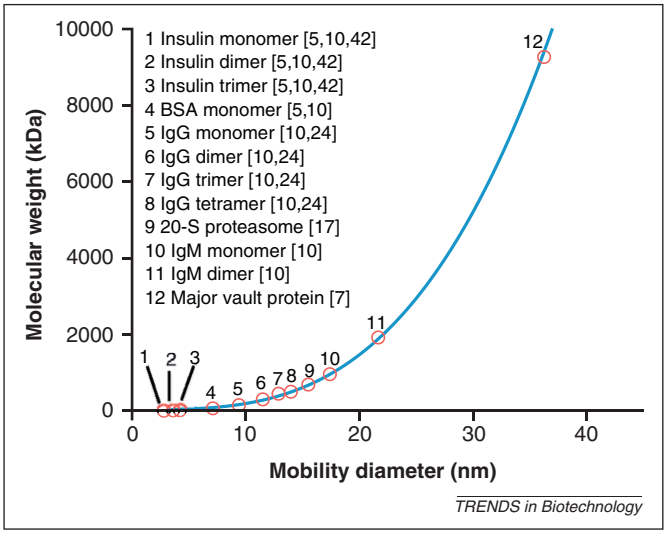

Figure 2. Electrospray–differential mobility analysis (ES–DMA) can be employed for proteins ranging from a few kDa up to thousands of kDa as demonstrated in this plot of molecular weight versus mobility diameter using data obtained from different groups. In this size range, there is an empirical correlation between the molecular weight and the mobility diameter as indicated by the blue bold line [15]. This molecular weight range far exceeds the range of most electrospray–mass spectrometry (ES–MS) applications (barring a few exceptions where ES–MS has been used to characterize viruses of several thousand kDa [67,68]). This correlation can be used to determine the molecular weight of protein oligomers unambiguously, although it should be kept in mind that different DMAs can yield slight differences in the mobility diameter (15%) [42].

validity of this correlation implies that proteins (especially non globular proteins) undergo structural changes and become spherical during the evaporation of the ES droplet. A recent study with GroEL, a 14-mer complex suggested partial collapse of the structure in the aerosol phase after the ES–DMA thus strengthening this hypothesis, although it should be noted that a 'neutralizer' was not used for charge reduction in this particular study [14].

ES–DMA has been used to resolve protein aggregates of DNase [29], insulin [27] and various immunoglobulins [16]. It has also been used to gain insight into the function of a number of protein complexes such as vault proteins [28], 20S proteasome [30], ErbB3[31], hemoglobin (Hb), Hemopure (a crosslinked Hb) [7] and for correlating heart disease risks with the size of lipoproteins [32]. A brief review of some of these results is available elsewhere [7].

The quantification of different oligomers of proteins has been reported for human antibodies [16], bovine serum albumin [5], hemoglobin [33] and 20-S proteasome complex [30]. One potentially confounding factor in these studies is adsorption of proteins to the ES capillary, which produces time variant size distributions [5,34]. Furthermore, studies suggest that proteins aggregate upon adsorption to different surfaces [35], however, recent evidence suggests that this effect does not significantly alter size distributions obtained with the ES–DMA [36].

Another potentially significant problem in the quantification of aggregates using ES–DMA, is 'droplet-induced aggregation' [37] also referred to as 'non-specific aggregation' by the ES–MS community [38]. During the aerosolization of nanoparticles (bio and non-bio alike) in ES, two or more monomers of a nanoparticle may exist in a droplet that, upon evaporation, will be incorrectly measured as an intrinsic aggregate in MS or DMA. This artifact can be minimized either by conducting measurements of proteins at low concentration, or by reducing the ES droplet volume [5,37,39]. To make ES–DMA useful to biopharmaceutical applications where many protein therapeutics are formulated at high concentrations, a statistical approach has recently been developed that permits one to correct for this undesired artifact [37]. A key feature of this statistical approach is that by measuring the relative oligomer mobility size distributions, one is able to work backwards to determine the absolute number concentration in solution. What is particularly attractive about this method is that by only measuring the relative oligomer concentrations, one eliminates the need for sample-specific calibration standards, or detailed analysis of transport losses [40].

ES–DMA can be used to determine the density of proteins. However, density determined using Equation 4 has been found to vary almost by a factor of two by different groups. Non-commercial DMAs yield protein densities close to liquid phase density (0.9–1.1 g/ml) [5,29,41], whereas commercial ES–DMAs yield densities close to 0.6 g/ml [7,15]. To explain this scatter, it has been hypothesized that the mobility diameters may depend on the geometric features of DMAs [13]. It is known that the mobility diameter obtained for same particles with different DMAs can vary by as much as 15% [42]. Applying uncertainty analysis on Equation 4, a 15% variation in mobility diameter results in ~45% variation in density, which partially explains this wide scatter of densities in the literature. The same rationale may also explain the scatter of densities found in PEGs [19,21].

Viruses and bacteriophages

As the threat of biological warfare increased in the late 20th century, a need to accurately and yet rapidly size and quantify viruses with high resolution led to the first reported use of ES–DMA for viruses in 1999 [43], although this application of ES–DMA had been first conceptualized in 1993 (Accession number: ADA337490). ES–DMA has been used to characterize enveloped (Accession number: ADA454377) [6,7,15,44,45] and naked viruses [43,45–51], as well as virus like particles (VLPs) [52] ranging in size from 22.5 nm (Accession number: ADA454377) to above 200 nm [6]. The reader can refer elsewhere for a comprehensive list of viruses characterized with ES–DMA [9].

Unlike proteins, Equation 4 cannot be used to correlate the molecular weight of viruses with mobility due to density differences of the different internal constituents of viruses [15]. By collecting viruses post-ES [46] and post-ES–DMA [6], it has been established that some viruses (e.g. MS2, λ) remain viable after the ES process, whereas others do not (e.g. T2, T4 [46] and TMV [6]). The latter also appear at mobility diameters smaller than expected, especially if the ES droplet sizes are smaller or comparable to these viruses. It has been speculated that electrical or mechanical perturbation during the ES evaporation process may disrupt the integrity of these viruses. That some viruses indeed break up during the ES process has also recently been corroborated with TMV [6].

Recently, to evaluate the accuracy of ES–DMA in measuring concentration, the viral concentration of MS2 (Accession number: ADA364117), T2 [46], T4 [46], PP7 and

PR772 [53] obtained with ES–DMA was compared to plaque assay, and was found to be linear over several orders of magnitude. In these studies it was assumed that the transport losses of these viruses were the same as gold nanoparticles (AuNPs) of approximately similar sizes (e.g. ~20 nm AuNPs were used determining transport losses of ~23 nm PP7), although this assumption may not always be valid (S. Guha *et al.*, unpublished). It has also been demonstrated that ES–DMA meets several of the requirements (such as specificity, linearity, precision and accuracy) set forth by the International Committee of Harmonisation (ICH). In this regard, ICH regulates the necessary characteristics required for validating analytical methods. Thus, this demonstration offers the possibility of ES–DMA's eventual use in biomanufacturing environments [53].

Nanoparticle–biomolecule conjugates

Gold nanoparticles (AuNPs) are being intensely studied for biosensing and health diagnostic applications in part because of the ease with which they can be surface functionalized. The adsorption of biomolecular ligands, such as nucleic acids and proteins, to AuNPs often leads to an increase in mobility diameter that can be measured using ES–DMA. This principle has been demonstrated with several different systems [44,54–62]. For example, ES–DMA has been used to characterize, and quantify surface coverage of single-strand DNA molecules on 10 nm gold nanoparticles [56]. Similar studies have been reported for self-assembled alkane thiol monolayers (SAMs) on 10 and 60 nm AuNPs [62]. This study found that the coverage of SAMs was independent of the size of the AuNPs. BSA was recently used as a model protein to study AuNP–protein interactions as a function of concentration and pH [55]. To further model the complexity inside human plasma where multicomponent species may be present, competitive adsorption–desorption of SAMs and PEGs on AuNPs has been successfully studied [59].

ES–DMA has also been used to characterize a variety of bimolecular complexes, such as oligomerization of subunits of ribonucleotide reductase in the presence of different functional groups [54] and triphosphates [57],

Box 3. Applications, advantages and limitations of ES–DMA

Applications

(i) Obtaining multimodal size distributions (particularly for spherical or nearly spherical particles) from ~3 nm to several hundred nanometers in a few minutes.
(ii) Determination of molecular weight of polymers and proteins using a correlation between molecular weight and mobility diameter [15]. Conversely, if the molecular weight is known, it can be used to determine the analyte density.
(iii) Kinetics of aggregation of nanoparticles, and bionanoparticles in liquids [26,27].
(iv) Quantifying ligand adsorption to bionanoparticles by determining increase in mobility diameter [44,59].
(v) Determination of absolute number concentration in liquid phase [40].
(vi) Quantifying protein adsorption and desorption on ES capillaries [34].

Advantages

(i) ES–DMA characterization is independent of particle type, and thus no prior information about the particle type is required. The use of charge neutralizers results in a reduction of the number of charge states per particle compared to ES–MS, and thus makes the data interpretation and the mobility spectra relatively simple to analyze [17]. ES–DMA operates under ambient pressure conditions and does not require sophisticated pumping. This latter operational characteristic also makes its interface to other instruments (such as counters, substrates and mass spectrometry) much easier.
(ii) ES–DMA has been routinely used to characterize particles over a broad size range (~3 nm to several hundred nanometers), and has also been validated with several independent liquid and gas phase techniques [14,21,23,24,27,44,45,52,53,74,75]. Indeed, ES–DMA was one of the primary tools in the recent development of NIST traceable nanoparticle size standards (https://www-s.nist.gov/srmors/view_report.cfm?srm=8011). Although the commercialized ES–DMA has been used up to several hundred nanometers, it can be used for characterizing particles up to ~2 μm, and thus its operational size range is significantly greater than both SEC and MS. It should be pointed out, however, that for micron sized particles, multiple charging and a decrease in resolution (at fixed flow rate) can pose difficulties. Multiple charging can be deconvoluted by using tandem DMA methods, analogous to MS–MS studies. [76]
(iii) The resolution of ES–DMA (even at less than 100:1) is better than either than SEC and DLS, and is comparable to that of AUC and FFF [26].
(iv) ES–DMA can be operated in a scanning mode [10] such that the total time of analysis is 2–4 min, and significantly shorter compared to several other methods. (e.g. SEC and FFF ~30 min; AUC ~3–6 h).
(v) ES–DMA requires small sample volumes (a few μls or less depending on time of analysis).
(vi) Relative to other methods, ES–DMA has high sensitivity. The lower limit of detection of ES–DMA is 1000-fold less than UV-Vis based detectors typically used in SEC, AUC and FFF [4]. In this regard, the lower limit of detection has been determined to be ~10^9 particles/ml for AuNPs [27,53].

Limitations

(i) Liquid phase techniques such as SEC, AUC, FFF and DLS are widely used by the biopharmaceutical industry for characterizing protein stability and aggregate formation. Most of these techniques are capable of analyzing high concentrations of proteins (10–100 mg/ml), in non-volatile buffers and at high ionic strengths (100–1000 mM). By contrast, ES artifacts [37] and instability limit the solution conditions to concentrations of a few hundred μg/ml [37] (protein and ES droplet volume specific), low ionic strength (<100 mM) and volatile buffers [5,24,46,62,73]. Furthermore, characterization of proteins from cell media require some preprocessing, such as dialysis, to prevent droplet-induced coagulation of the analyte and heterogeneous media.
(ii) The uncertainty in measurements of ES–DMA is typically ± 0.3 nm from a size range of a few nanometers [27] to at least ~100 nm [53,64] and appears to be independent of resolution. However, this uncertainty sometimes may not be adequate to distinguish proteins with slight differences in molecular weight. For example, two proteins with molecular weights of 145 kDa and 150 kDa would have predicted [15,64] mobility diameters of 9.3 nm and 9.4 nm, respectively. These values are within the uncertainty, and thus ES–DMA cannot distinguish between these two proteins. This limitation has been reported for certain cases [75,77]. By contrast, a typical ES–MS can easily distinguish differences in molecular weights of a few daltons.
(iii) A typical commercially available ES–DMA and CPC detection system will cost ~$100 000 (USD) and thus is a greater financial impediment relative to gel electrophoresis, capillary electrophoresis, SEC, DLS and FFF [25,37]. However, recent developments in DMA technology may potentially reduce the price [78].

PEGylated-Von Willebrand factor (VWF) protein [58], quantification of the coverage of antibodies (8F5) on human common cold virus [44] and quantum dots (QDs) on bacteriophages [60,61].

Two approaches are used to quantify adsorbed ligand (usually peptides and or proteins) on a primary particle (such as AuNP, virus or protein). One approach is based on the increase in projected surface area due to adsorption of ligand [55,60,61].

$$N_{ligand} = \pi \left(\frac{d^2_{conjugate} - d^2_{primary}}{4A_{ligand}} \right)^2 \quad (5)$$

N_{ligand} is defined as the number of ligands per primary particle, $d_{conjugate}$ and $d_{primary}$ are the mobility diameters of the conjugates and primary particles, respectively, and A_{ligand} is the projected area of the ligand in liquid phase. The above equation has been employed for quantifying surface coverage of polymers and proteins on AuNPs, as well as QDs on phages. The other approach is to quantify the increase in volume due to adsorption of the ligand [44]:

$$N_{ligand} = \frac{d^3_{conjugate} - d^3_{primary}}{d^3_{ligand}} \quad (6)$$

where d_{ligand} is the mobility diameter of the ligand. This has been used for quantifying the number of 8F5 antibodies that bind to human common cold virus, and corroborated with cryo-microscopy [44]. For the same mobility diameter increase of a primary particle, each of these approaches gives different ligand coverages, with Equation 6 always yield higher coverages for ligand sizes >2 nm. Further systematic studies and comparison with several other orthogonal techniques are required to determine which approach provides more accurate values. It should be pointed out that both equations assume that a ligand, upon adsorption, does not change size (or conformation).

Concluding remarks

The rapid increase in publications employing ES–DMA to a variety of bionanoparticles suggests it will play an increasing important role as a research tool, and possibly as a process analytical tool. Although it has certain limitations, ES–DMA offers the potential for rapid, high resolution and accurate size characterization in a multi-component environment (Box 3).

One clear trend is the coupling of ES–DMA to other analytical methods. For example, placing ES–DMA-(–CPC) after SEC can be useful to the biopharmaceutical industry with respect to characterization and detection of protein aggregates, similar to SEC–ES–CPC systems as demonstrated previously [4]. ES–DMA has been used in conjunction with aerosol samplers [6] allowing the aerosolized particles to be re-suspended in the liquid phase after the DMA. The particles can then be probed for biological or functional activity post-ES or post-ES–DMA. Coupling of MS with ES–DMA offers the possibility to understand large protein complexes by first size selecting them with a DMA followed by measurement and fragmentation by MS [13,24]. ES–DMA can also be coupled with inductively coupled plasma MS (ICPMS) to enable size resolved elemental composition [63]. It can also be coupled to aerosol particle mass analyzers (APM) [64] that utilizes the balance of electrical forces and centrifugal forces to determine the mass of particles. Although mass has been deduced using the ES–DMA only for spherical particles, ES–DMA–APM has the potential to determine the mass of non-spherical particles, particularly large protein and virus aggregates, which concomitantly can provide information about the morphology of these aggregates. Thus, the hyphenation of ES–DMA with other techniques promises to bring more answers to important questions in the realm of biotechnology.

Acknowledgments

We have attempted to include all recent literature on applications of the ES–DMA and exclusion of any relevant work is inadvertent. We would also like to thank the editor and the referees for contributing to the quality of this review, and Stanley Kaufman and Christopher Hogan for sharing the data from their papers with us. Reference to commercial equipment or supplies does not imply endorsement by the University of Maryland or the National Institute of Standards and Technology.

References

1 Chen, D.R. and Pui, D.Y.H. (2010) Electrospray and its medical applications. In *Nanoparticles in Medicine and Environment: Inhalation and Health Effects* (Marijinissen, J. and Gradon, L., eds), pp. 59–75, Springer Science
2 Fenn, J.H. *et al.* (1989) Electrospray ionization for mass spectrometry of large biomolecules. *Science* 246, 64–71
3 Flagan, R.C. (1998) History of electrical aerosol measurements. *Aerosol Sci. Technol.* 28, 301–380
4 Lewis, K.C. *et al.* (1994) Electrospray-condensation particle counter: a molecule-counting LC detector for macromolecules. *Anal. Chem.* 66, 2285–2292
5 Kaufman, S.L. *et al.* (1996) Macromolecule analysis based on electrophoretic mobility in air: globular proteins. *Anal. Chem.* 68, 1895–1904
6 Allmaier, G. *et al.* (2008) Nano ES GEMMA and PDMA, new tools for the analysis of nanobioparticles-protein complexes, lipoparticles, and viruses. *J. Am. Soc. Mass Spectrom.* 19, 1062–1068
7 Kaddis, C.S. and Loo, J.A. (2007) Native protein MS and ion mobility large flying proteins with ESI. *Anal. Chem.* 79, 1778–1784
8 Allmaier, G. *et al.* (2011) Parallel differential mobility analysis for electrostatic characterization and manipulation of nanoparticles and viruses. *Trends Anal. Chem.* 30, 123–132
9 Pease III, L.F. (2012) Physical analysis of virus particles using electrospray differential mobility analysis. *Trends Biotech.* 30, 216–224
10 Flagan, R.C. (2008) Differential mobility analysis of aerosols: a tutorial. *KONA Particle Powder J.* 26, 254–268
11 Kim, S.H *et al.* (2007) Understanding ion-mobility and transport properties of aerosol nanowires. *J. Aerosol Sci.* 38, 823–842
12 Uetrecht, C. *et al.* (2010) Ion mobility mass spectrometry of proteins and protein assemblies. *Chem. Soc. Rev.* 39, 1633–1655
13 Hogan, C.J., Jr and de la Mora, J.F. (2011) Ion mobility measurements of nondenatured 12-150 kDa proteins and protein multimers by tandem differential mobility analysis-mass spectrometry (DMA-MS). *J. Am. Soc. Mass Spectrom.* 22, 158–172
14 Hogan, C.J., Jr *et al.* (2011) Tandem differential mobility analysis-mass spectrometry reveals partial gas-phase collapse of the GroEL complex. *J. Phys. Chem. B* 115, 3614–3621
15 Bacher, G. *et al.* (2001) Charge-reduced nano electrospray ionization combined with differential mobility analysis of peptides, proteins, glycoproteins, noncovalent protein complexes and viruses. *J. Mass Spectrom.* 36, 1038–1052
16 Pease, L.F. *et al.* (2008) Determination of protein aggregation with differential mobility analysis: application to IgG antibody. *Biotech. Bioeng.* 101, 1214–1222
17 Scalf, M. *et al.* (1999) Controlling charge state of large ions. *Science* 283, 194–197

18 Mouradian, S. *et al.* (1997) DNA analysis using an electrospray scanning mobility particle sizer. *Anal. Chem.* 69, 919–925
19 Saucy, D.A. *et al.* (2004) Mass analysis of water-soluble polymers by mobility measurement of charge-reduced ions generated by electrosprays. *Anal. Chem.* 76, 1045–1053
20 Ku, B.K. and de la Mora, J.F. (2004) Mass distribution measurement of water-insoluble polymers by charge-reduced electrospray mobility analysis. *Anal. Chem.* 76, 814–822
21 Kemptner, J. *et al.* (2010) GEMMA and MALDI-TOF MS of reactive PEGs for pharmaceutical applications. *J. Pharm. Biomed. Anal.* 52, 432–437
22 Mordas, G. *et al.* (2008) On operation of the ultra-fine water-based CPC TSI 3786 and comparison with other TSI models (TSI 3776, TSI 3772, TSI 3025, TSI 3010, TSI 3007). *Aerosol Sci. Tech.* 42, 152–158
23 Muller, R. *et al.* (2007) Determination of molecular weight, particle size, and density of high number generation PAMAM dendrimers using MALDI-TOF-MS and nES-GEMMA. *Macromolecules* 40, 5599–5605
24 Anumolu, R. *et al.* (2011) Fabrication of highly uniform nanoparticles from recombinant silk-elastin-like protein polymers for therapeutic agent delivery. *ACS Nano* 5, 5374–5382
25 Wang, W. and Roberts, C.J. (2010) *Aggregation of Therapeutic Proteins*, John Wiley & Sons
26 Guha, S. *et al.* (2012) Electrospray differential mobility analysis as an orthogonal tool to size exclusion chromatography for characterization of protein aggregates. *J. Pharm. Sci.* DOI: 10.1002/jps.23097
27 Pease, L.F. *et al.* (2010) Probing the nucleus model for oligomer formation during insulin amyloid fibrillogenesis. *Biophys. J.* 99, 3979–3985
28 Poderycki, M.J. *et al.* (2006) The vault exterior shell is a dynamic structure that allows incorporation of vault-associated proteins into its interior. *Biochemistry* 45, 12184–12193
29 Kaufman, S.L. (1998) Analysis of biomolecules using electrospray and nanoparticle methods: the gas-phase electrophoretic mobility molecular analyzer (GEMMA). *Aerosol Sci.* 29, 537–552
30 Loo, J.A. *et al.* (2005) Electrospray ionization mass spectrometry and ion mobility analysis of the 20S proteasome complex. *J. Am. Soc. Mass Spectrom.* 16, 998–1008
31 Kani, K. *et al.* (2005) Oligomers of ERBB3 have two distinct interfaces that differ in their sensitivity to disruption by heregulin. *J. Biol. Chem.* 280, 8238–8247
32 Caulfield, M.P. *et al.* (2008) Direct determination of lipoprotein particle sizes and concentrations by ion mobility analysis. *Clin. Chem.* 54, 1307–1316
33 Kaufman, S.L. *et al.* (1998) Analysis of a 3.6-MDa hexagonal bilayer hemoglobin from *Lumbricus terrestris* using a gas-phase electrophoretic mobility molecular analyzer. *Anal. Biochem.* 259, 195–202
34 Guha, S. *et al.* (2011) Characterizing the adsorption of proteins on glass capillary surfaces using electrospray-differential mobility analysis (ES-DMA). *Langmuir* 27, 13008–13014
35 Mulheran, P.A. *et al.* (2008) Mechanisms and dynamics of protein clustering on a solid surface. *Phys. Rev. Lett.* 100, 068102(1)–068102(4)
36 Guha, S. *et al.* (2012) Protein adsorption-desorption on electrospray capillary walls – No influence on aggregate distribution. *J. Colloid Interface Sci.* DOI: 10.1016/j.jcis.2012.03.059
37 Li, M.D. *et al.* (2011) Quantification and compensation of nonspecific analyte aggregation in electrospray sampling. *Aerosol Sci. Tech.* 45, 849–860
38 Lane, L.A. *et al.* (2009) A Monte Carlo approach for assessing the specificity of protein oligomers observed in nano-electrospray mass spectra. *Int. J. Mass Spectrom.* 283, 169–177
39 Pease, L.F. (2010) Optimizing the yield and selectivity of high purity nanoparticle clusters. *J. Nanoparticle Res.* 13, 2157–2172
40 Li, M.D. *et al.* (2011) Method for determining absolute number concentration of nanoparticles from electrospray sources. *Langmuir* 27, 14732–14739
41 Maißer, A. *et al.* (2011) Determination of gas phase protein ion densities via ion mobility analysis with charge reduction. *Phys. Chem. Chem. Phys.* 13, 21630–21641
42 Laschober, C. *et al.* (2007) Comparison of various nano-differential mobility analysers (nDMAs) applying globular proteins. *J. Exp. Nanoscience* 2, 291–301
43 Wick, C.H. and McCubbin, P.E. (1999) Characterization of purified MS2 bacteriophage by physical counting methodology used in the integrated virus detection system (IVDS). *Toxicol. Mech. Methods* 9, 245–252
44 Laschober, C. *et al.* (2008) Gas-phase electrophoretic molecular mobility analysis of size and stoichiometry of complexes of a common cold virus with antibody and soluble receptor molecules. *Anal. Chem.* 80, 2261–2264
45 Thomas, J.J. *et al.* (2004) Electrospray ion mobility spectrometry of intact viruses. *Spectroscopy* 18, 31–36
46 Hogan, C.J. *et al.* (2006) Charge reduced electrospray size spectrometry of mega- and gigadalton complexes: whole viruses and virus fragments. *Anal. Chem.* 78, 844–852
47 Cole, K.D. *et al.* (2009) Particle concentration measurement of virus samples using electrospray differential mobility analysis and quantitative amino acid analysis. *J. Chromatogr. A* 1216, 5715–5722
48 Pease, L.F. *et al.* (2011) Rapid physical characterization of icosahedral virus ultrastructure, stability and integrity using electrospray differential mobility analysis. *Anal. Chem.* 83, 1753–1759
49 Lute, S. *et al.* (2010) A consensus rating method for small virus-retentive filters. I. Method Development. *PDA J. Pharm. Sci. Tech.* 62, 318–333
50 Wick, C.H. *et al.* (2007) Mass spectrometry and integrated virus detection system characterization of MS2 bacteriophage. *Toxicol. Mech. Methods* 17, 241–254
51 Kuzmanovic, D.A. *et al.* (2008) A novel application of small-angle scattering techniques: quality assurance testing of virus quantification technology. *Radiat. Phys. Chem.* 77, 215–224
52 Pease, L.F. *et al.* (2009) Quantitative characterization of virus-like particles by asymmetrical flow field flow fractionation, electrospray differential mobility analysis, and transmission electron microscopy. *Biotech. Bioeng.* 102, 845–855
53 Guha, S. *et al.* (2011) Evaluation of electrospray differential mobility analysis for virus particle analysis: Potential applications in biomanufacturing. *J. Virol. Methods* 178, 201–208
54 Crona, M. *et al.* (2011) Assembly of a fragmented ribonucleotide reductase by protein interaction domains derived from a mobile genetic element. *Nucleic Acids Res.* 39, 1381–1389
55 Tsai, D.H. *et al.* (2011) Adsorption and conformation of serum albumin protein on gold nanoparticles investigated using dimensional measurements and in situ spectroscopic methods. *Langmuir* 27, 2464–2477
56 Pease, L.F. *et al.* (2007) Quantifying the surface coverage of conjugate molecules on functionalized nanoparticles. *J. Phys. Chem. C* 111, 17155–17157
57 Rofuogaran, R. *et al.* (2008) Oligomerization status directs overall activity regulation of the *Escherichia coli* class Ia ribonucleotide reductase. *J. Biol. Chem.* 283, 35310–35318
58 Seyfried, B.K. *et al.* (2010) PEGylated recombinant von Willebrand factor analyzed by means of MALDI-TOF-MS. *CGE-on-a-chip and nES-GEMMA. Int. J. Mass Spect.* 305, 157–163
59 Tsai, D.H. *et al.* (2010) Competitive adsorption of thiolated polyethylene glycol and mercaptopropionic acid on gold nanoparticles measured by physical characterization methods. *Langmuir* 26, 10325–10333
60 Yim, P.B. *et al.* (2009) Quantitative characterization of quantum dot-labeled lambda phage for *Escherichia coli* detection. *Biotechnol. Bioeng.* 104, 1059–1067
61 Pease, L.F. *et al.* (2010) Structural analysis of soft multicomponent nanoparticle clusters. *ACS Nano* 4, 6982–6988
62 Tsai, D.H. *et al.* (2008) Gas-phase ion-mobility characterization of SAM-functionalized Au nanoparticles. *Langmuir* 24, 8483–8490
63 Carazzone, C. *et al.* (2008) Nanoelectrospray ion mobility spectrometry online with inductively coupled plasma-mass spectrometry for sizing large proteins, DNA, and nanoparticles. *Anal. Chem.* 80, 5812–5818
64 Lall, A.A. *et al.* (2009) Online nanoparticle mass measurement by combined aerosol particle mass analyzer and differential mobility analyzer: comparison of theory and measurements. *Aerosol Sci. Technol.* 42, 1075–1083
65 El-Aneed, A. *et al.* (2009) Mass spectrometry, review of the basics: electrospray, maldi, and commonly used mass analyzers. *Appl. Spectrosc. Rev.* 44, 210–230

66 Kebarle, P. and Peschke, M. (2000) On the mechanisms by which the charged droplets produced by electrospray lead to gas phase ions. *Anal. Chim. Acta* 406, 11–35
67 Tito, M.A. *et al.* (2000) Electrospray time-of-flight mass spectrometry of the intact MS2 virus capsid. *J. Am. Chem. Soc.* 122, 3550–3551
68 Uetrecht, C. *et al.* (2008) High-resolution mass spectrometry of viral assemblies: molecular composition and stability of dimorphic hepatitis B virus capsids. *Proc. Natl. Acad. Sci. U.S.A.* 105, 9216–9220
69 Stolzenberg, M.R. and McMurry, P.H. (2008) Equations governing single and tandem DMA configurations and a new lognormal approximation to the transfer function. *Aerosol Sci. Tech.* 42, 421–432
70 Martínez-Lozano, P. and de la Mora, J.F. (2006) Resolution improvements of a nano-DMA operating transonically. *J. Aerosol Sci.* 37, 500–512
71 Kulkarni, P. *et al.* (2011) *Condensation Particle Counters in Aerosol Measurement: Principle, Techniques and Applications*, (3rd edn), John Wiley & Sons
72 Jiang, J. *et al.* (2011) Electrical mobility spectrometer using a diethylene glycol condensation particle counter for measurement of aerosol size distributions down to 1 nm. *Aerosol Sci. Tech.* 45, 510–521
73 Kapellios, E.A. *et al.* (2011) Using nanoelectrospray ion mobility spectrometry (GEMMA) to determine the size and relative molecular mass of proteins and protein assemblies: a comparison with MALLS and QELS. *Anal. Bioanal. Chem.* 399, 2421–2433
74 Pease, L.F. *et al.* (2009) Length distribution of single-walled carbon nanotubes in aqueous suspension measured by electrospray differential mobility analysis. *Small* 5, 2894–2901
75 Kemptner, J. *et al.* (2010) A comparison of nano-electrospray gas-phase electrophoretic mobility macromolecular analysis and matrix-assisted laser desorption/ionization linear time-of-flight mass spectrometry for the characterization of the recombinant coagulation glycoprotein von Willebrand factor. *Rapid Commun. Mass Spectrom.* 24, 761–767
76 Kim, S.H. *et al.* (2005) Method of measuring charge distribution of nanosized aerosols. *J. Colloid Interface Sci.* 282, 46–57
77 Guha, S. *et al.* (2010) Electrospray-differential mobility analysis (ES-DMA) for characterization of heat induced antibody aggregates. In *IFMBE Proceedings, 26th Biomedical Engineering Conference* (Herold, K.E. and Vossoughi, J., eds), pp. 232–235
78 Mei, F. *et al.* (2011) A cost-effective differential mobility analyzer (cDMA) for multiple DMA column applications. *J. Aerosol Sci.* 42, 462–473